JOURNAL OF Materials CHEMISTRY

Spectroscopic study on strongly luminescent Nd(III) exchanged zeolite: TMA^+-containing FAU type zeolite as a suitable host for ship-in-bottle synthesis

Munenori Ryo,[a] Yuji Wada,[a] Tatsuya Okubo,[b] Toru Nakazawa,[c] Yasuchika Hasegawa[a] and Shozo Yanagida*[a]

[a] *Material and Life Science, Graduate School of engineering, Osaka University, Yamada-oka, Suita, Osaka 565-0871, Japan. E-mail: yanagida@chem.eng.osaka-u.ac.jp; Tel: +81-6-6879-7924; Fax: +81-6-6879-7875; http://www.mls.eng.osaka-u.ac.jp/~mol_pro*

[b] *PREST, JST and Department of Chemical System Engineering, The University of Tokyo, Bunkyo-ku, Tokyo 113-8656, Japan*

[c] *Department of Chemical System Engineering, The University of Tokyo, Bunkyo-ku, Tokyo 113-8656, Japan*

Received 3rd December 2001, Accepted 28th March 2002
First published as an Advance Article on the web 29th April 2002

Enhanced emission from intrazeolite Nd^{3+} was investigated by using bis(perfluoromethanesulfonyl)aminate (PMS) as a low vibrational ligand of the ion and TMA^+-containing FAU zeolite nanocrystallite (TMA–nano-FAU) as a host matrix. Treatments such as deuteration, and thermal treatments at high temperatures were ineffective for the strong emission of Nd^{3+} within this zeolite. The high-resolution emission and excitation spectra suggested that the environment of Nd^{3+} in the zeolite was more homogeneous than that in a glass matrix, and intrazeolitic emissive Nd^{3+} ions consisted of at least two species. The diffuse reflectance spectra revealed that the strong emission was attributed to the PMS ligands that eliminated hydroxy groups from the vicinity of the ion. On the other hand, thermal treatment at high temperatures induced emission of Nd^{3+}-exchanged Na–micro-FAU. Judd–Ofelt analysis revealed that the difference of the emission property between TMA–nano- and Na–micro-FAU zeolites depended on whether the cations migrated to the inner cages or not: in the former case, the ligation of PMS with the Nd^{3+} ion occurred easily, because the ions remained in the super cages without migrating into inner cages due to the hindrance of TMA^+ occupying in the sodalite cages. In the latter case, the ligation was suppressed because of the Nd^{3+} ions migrated into the inner cages from the supercages.

Introduction

Nd^{3+}-containing systems are regarded as the most popular infrared luminescent materials for application in laser systems. Developing a strongly luminescent Nd^{3+} center in organic media is attractive aim because of its applicability to organic liquid lasers,[1] optical-fiber polymers,[2] organic electroluminscent devices,[3] and near-infrared immunoassays. In general, effective luminescence of Nd^{3+} was regarded as being almost impossible in organic solvents due to the fast relaxation of its excitation energy through nonradiative vibrational excitation.[4–6] In addition, the excitation migration caused by diffusional collision between Nd^{3+} ions is unavoidable in liquid matrices.[7–9] The emission of Nd^{3+} can be observed by excluding high vibrational bonds such as C–H and O–H from the ligands and the surroundings[10–13] and increasing the distance between the emitting centers by ligating with long perfluoroalkyl chains.[14,15]

Zeolites play indispensable roles in many technological and economical applications. Of primary importance are their uses as catalysts and molecular sieves. Recently, zeolites have attracted scientists' interests as hosts of photochemically or optically active guests for constructing novel materials designed at the nanosize level.[16–21] A series of zeolites should be suitable host materials for the efficient near-infrared luminescence of rare earth ions, because their framework consists of low vibrational chemical bonds, Si–O–Si and Si–O–Al, and their pores have the ability to locate the cations separately.

Although luminescence of intrazeolite rare earth ions has been utilized mostly as an analytical tool for the topological assignment of ions to specific sites in these lattices,[22–27] their potential uses as new emitting materials have only been investigated recently.[28–35] The studies were mainly focused on Eu^{3+} or Tb^{3+} exchanged zeolites, but there were no successful reports on near-IR emission of rare earth ions such as Nd^{3+} and Er^{3+}, except for a study by Rocha *et al.*[34] They succeeded in observing strong luminescence of Er^{3+}-doped narsarsukite, which was obtained from ETS-10 by a phase transformation under calcination at high temperatures in excess of *ca.* 973 K. Unobservable near-IR emission of rare earth ions included in zeolites should be attributed to the existence of adsorbed and/or coordinated water to exchanged cations and silanol groups in the cages, causing energy transfer through vibrational excitation as pointed out for the emission of Eu^{3+}-exchanged zeolites.[25]

Zeolites are attractive hosts for efficient near-IR luminescence of rare earth ions because the zeolites consist of a low vibrational framework and they possess the ability to locate the ions separately, if water molecules and silanol groups in the pores are removed. Calcination of the zeolites at high temperatures is regarded as a method for excluding coordinating water. On the other hand, Alvaro *et al.* had reported that luminescence of intrazeolite Eu^{3+} was longer lived by using organic ligands such as 2,2′-biprydine, and this long emission may be attributed to the exclusion of water and silanol groups from the vicinity of the ion by the ligand.[31]

From the viewpoint of applicability of strong emissive Nd^{3+}

 DOI: 10.1039/b111032m

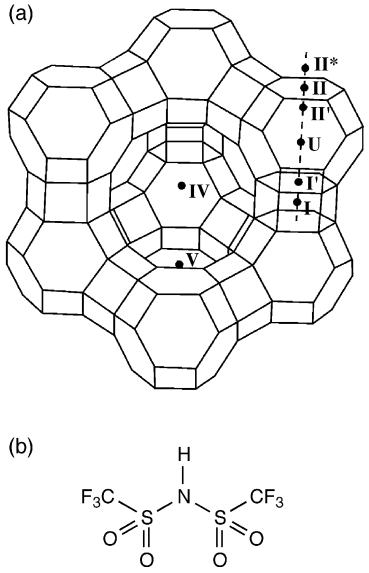

Fig. 1 (a) Structure of FAU type zeolite. (b) Chemical structure of bis(perfluoromethanesulfonyl)amine (PMS).

centers in organic media, we had given attention to zeolite nanocrystallites.[36–39] Calcination at high temperatures is undesirable especially for the nanocrystallites because it induces their aggregation. Then, we tried to enhance the near-IR emission efficiency of Nd^{3+} by ligating it with bis(perfluoromethanesulfonyl)aminate (PMS), as the lowest vibrational structure of the reported ligands,[15] in the cages of the zeolite. We had selected the highly crystalline FAU type zeolite,[39] having sufficiently large pores for the ligand PMS to diffuse (the structures are depicted in Fig. 1). As a result, we successfully observed near-IR emission of Nd^{3+} in the cages of the zeolite with the highest quantum yield ($9.5 \pm 1.0\%$) in organic media for the first time.[40] Thus, we concluded that for near-IR emission of the rare earth ion, the zeolite was an excellent host matrix when combined with an appropriate ligand such as PMS.

In the present report, we have examined the optical properties of the Nd^{3+}-exchanged zeolites as dried powder samples. The relationship between the emission intensity and the intrazeolite environment of Nd^{3+} is discussed on the basis of the spectroscopic methods including high-resolution emission and excitation spectra, diffuse reflectance spectra, and Judd–Ofelt analysis.[41]

Experimental

I. Zeolites

Synthesis of the nanocrystalline zeolite (TMA–nano-FAU) was carried out according to a method reported in the literature using a clear solution containing a system of composition 3.4 SiO_2–1.7 Al_2O_3–2.3 $(TMA)_2O$–0.1 NaCl–300 H_2O. The procedure was as follows. Aluminium powder (99.9%, Nilaco) and NaCl (Wako) were dissolved in a tetramethylammonium hydroxide (15% aq, Wako) solution. This solution was then filtered through a 0.2 μm membrane filter. A measured amount of tetraethylorthosilicate (Wako) was added dropwise to the solution under stirring. After 48 hours of aging, the solution was heated in an air-circulated oven at 373 K for 14 days. The resulting solid was separated by centrifugation (10000 G) for 90 min, washed by dialysis with deionized water until the pH of the colloidal suspension containing the nanocrystalline reached about 7. The nanocrystallites were separated by centrifugation for 90 min and dried at 358 K.

Na–micro-FAU zeolite (Si/Al = 2.4) was supplied by Catalysis Society of Japan (JRC-Z-Y4.8).

II. Preparation of optical samples

Nd^{3+}-exchanged zeolites were prepared by adding the synthesized nano-sized zeolite or the micro-sized zeolite to a 0.1 M aqueous solution of $NdCl_3 \cdot 6H_2O$ followed by stirring at 373 K for 24 h. After the products were removed by centrifugation, they were washed with deionised water, and dried in air at 358 K.

The Nd^{3+}-exchanged zeolites were degassed at different temperatures for 30 min, subsequently treated with D_2O or PMS (Fluka), which gave the lower vibrational environment to Nd^{3+} within the zeolites. The deuteration was performed by exposing the zeolites to D_2O vapor at 423 K for 10 min three times. The PMS treatment was performed by exposing the zeolites to PMS vapor at 373 K for 1 hour. The resulting samples were degassed at different temperatures for 30 min, and then sealed under vacuum. This sequence was carried out in a vacuum line without exposing the zeolites to the atmosphere.

III. Measurements

The XRD pattern of the synthesized zeolite was recorded on a MAC Science Co., Ltd. MXP3 system using Ni-filtered Cu Kα radiation (40 kV and 40 mA). FE-SEM (HITACHI S-900) was applied to observe the morphology and the particle size of the zeolite. The disappearance of TMA cations by Nd^{3+} exchange in the synthesized zeolite was confirmed by differential thermal analysis (DSC, Shimadzu DSC-60). The percentage of Nd^{3+} exchange was determined by ICP (Shimadzu ICPS-IV). The amount of adsorbed ligand, PMS, was determined using the amounts of carbon and nitrogen contained in the zeolite obtained by combustion chemical analysis.

Emission and excitation spectra were obtained with a JASCO SS-25 using a liquid nitrogen-cooled Ge detector. Diffuse reflectance spectra (DR spectra) were recorded on JASCO V-570 spectrophotometer having an integral sphere accessory in the 400–1500 nm spectral range. Judd–Ofelt analysis is difficult by using diffusion reflectance spectra, because the concentration and optical pathlength are necessary. In our system, the Nd^{3+} concentration was 12×10^{20} cm^{-3} (calculated by the contents of Nd^{3+} in the FAU zeolite and the cell constant of the zeolite), but the optical pathlength was unknown. We carried out Judd–Ofelt analyses by assuming that the optical pathlength was 0.01 cm. Thus, the obtained parameters were not absolute values. However, it was not wrong to compare these obtained parameters at least within our data when regarded as relative values, because the concentration and optical pathlength were constant in all cases. The reduced matrix elements of the unit tensor operator and the six integrated adsorption band intensities at λ = 400–900 nm for Judd–Ofelt analysis were the same as described before.[41]

Results and discussion

I. Characterization

The XRD pattern showed that the synthesized zeolite consisted of FAU (90 wt%) and LTA (10 wt%). This sample was denoted as TMA–nano-FAU, because it included TMA^+ originating from the synthetic procedures. In an FE-SEM image of the zeolite, octahedral crystals of 50–80 nm and cubic crystals of 70–130 nm could be observed, which were attributed to the characteristic morphologies of FAU and LTA, respectively. In the DSC curve (Fig. 2a), the peaks at 623 K and 773 K were attributed to decomposition of TMA^+ ions in the supercages and the sodalite cages, respectively.[42] After Nd^{3+} exchange, the

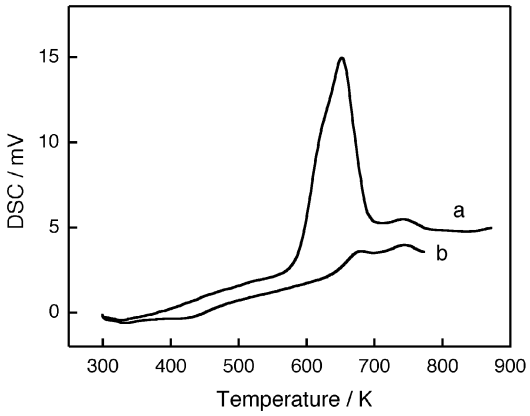

Fig. 2 DSC curves of synthesized TMA–nano-FAU zeolite nanocrystallites (a) before and (b) after exchange by Nd^{3+}.

peak at 623 K disappeared (Fig. 2b). This suggests that the TMA^+ ions in the supercages were exchanged by Nd^{3+} but the TMA^+ in the sodalite cages remained without being exchanged by Nd^{3+}. The Si/Al ratio of the TMA–nano-FAU zeolite was determined to be 2.0 by ICP measurements. The numbers of Nd^{3+} ions per unit cell were also determined to be 14.3 and 14.4 for TMA–nano- and Na–micro-FAU zeolites, respectively.

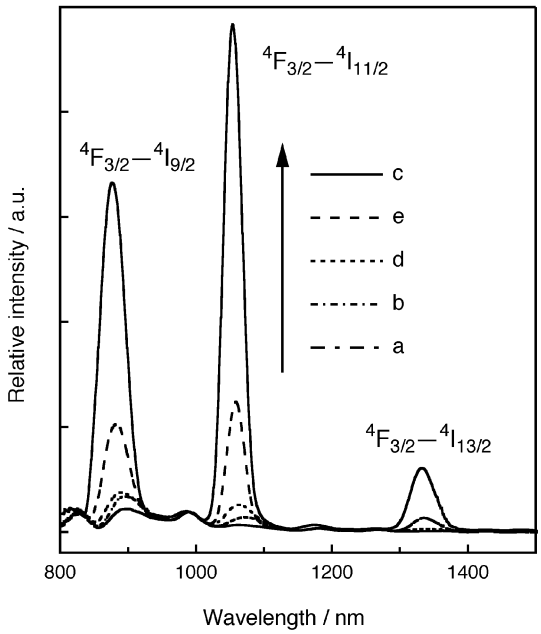

Fig. 3 Emission spectra of Nd^{3+}-exchanged TMA–nano-FAU zeolites prepared under different conditions. The excitation wavelength was 585 nm. The sample names are listed in Table 1.

II. Emission properties

For measurements of the emission spectra, the Nd^{3+}-exchanged TMA–nano-FAU zeolites were degassed, deuterated, or treated with PMS. The prepared zeoites are listed together with the preparation conditions in Table 1. Their emission spectra are depicted in Fig. 3. Under irradiation at 585 nm corresponding to the $^4I_{9/2}$–$^4G_{7/2}$ transition of Nd^{3+}, only the zeolites treated with PMS (sample c, d, e) gave luminescence attributed to the f–f transitions of Nd^{3+}. The spectra observed for the dueterated samples (a and b) were due to the scattered light because these were the same as that for TMA–nano-FAU. The PMS treatment was requisite for obtaining the emission of Nd^{3+} in the cage of TMA–nano-FAU zeolite. This should be attributed to replacement of water molecules coordinating to the ions by the ligands. It should be pointed out that the strongest emission intensity was obtained for sample c that was prepared under mild conditions and had a higher ratio of PMS/Nd^{3+} than the others.

Nd^{3+}-exchanged Na–micro-FAU zeolites were prepared as listed in Table 2. Their emission spectra are depicted in Fig. 4. The zeolites heated at higher temperatures than 523 K showed the emission. The treatment with PMS induced the emission even for the sample heated at 423 K (sample l). The enhanced emission by heating at high temperatures must be due to the loss of water and the migration of the Nd^{3+} ions from the supercages into the narrow cages (sodalite cages or hexagonal prisms).[26,33] No emission was observed for the TMA–nano-FAU zeolite heated at 573 K (sample b in Fig. 3). The difference in the emission behavior between the two zeolites after the treatment at high temperatures is considered to be due to the different positions of Nd^{3+} ions: Nd^{3+} ions migrate to the

Table 1 Nd^{3+}-exchanged TMA–nano-FAU zeolites prepared for luminescence measurements and relative intensity of the $^4F_{3/2}$–$^4I_{11/2}$ transition

Sample	Temperature of dehydration/K	PMS treatment	Deuteration	Temperature of degassing/K	PMS/Nd^{3+} ratio	Relative intensity[a]
a	423	—	done	423	—	—
b	573	—	done	573	—	—
c	423	done	—	423	1.5	12.5
d	423	done	—	573	0.97	3.3
e	573	done	—	423	0.57	1

[a]Relative intensity of the $^4F_{3/2}$–$^4I_{11/2}$ transition. The values were normalized by the intensity of sample e.

Table 2 Nd^{3+}-exchanged Na–micro-FAU zeolites prepared for luminescence measurements and relative intensity of the $^4F_{3/2}$–$^4I_{11/2}$ transition

Sample	Temperature of dehydration/K	PMS treatment	Deuteration	Temperature of degassing/K	PMS/Nd^{3+} ratio	Relative intensity[a]
f	423	—	done	423	—	—
g	473	—	—	—	—	—
h	523	—	—	—	—	1
i	573	—	—	—	—	4.6
j	623	—	—	—	—	5.8
k	673	—	—	—	—	8.0
l	423	done	—	423	1.6	2.6

[a]Relative intensity of the $^4F_{3/2}$–$^4I_{11/2}$ transition. The values were normalized by the intensity of sample h.

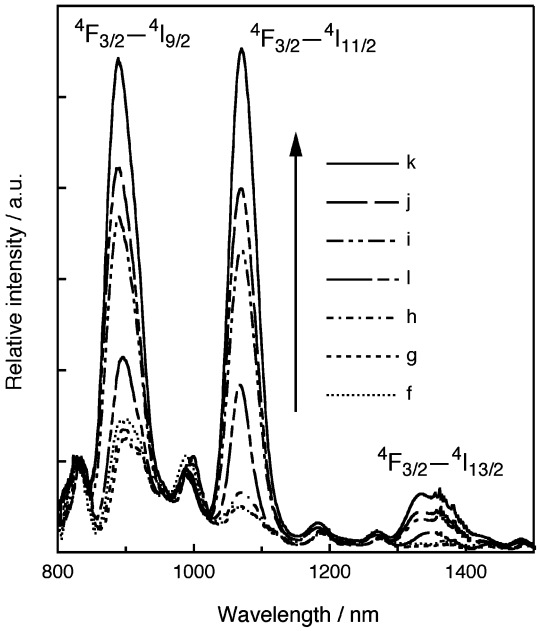

Fig. 4 Emission spectra of Nd^{3+}-exchanged Na–micro-FAU zeolites prepared under different conditions. The excitation wavelength was 585 nm. The sample names are listed in Table 2.

narrow cages in Na–micro-FAU but do not in TMA–nano-FAU due to the steric hindrance of TMA^+ present in the narrow cages. The emission intensity of Nd^{3+} in Na–micro-FAU zeolite treated with PMS was lower than that of the zeolite heated at 573 K, in contrast to the case of TMA–nano-FAU. This also may be related to the cation migration as discussed below.

We succeeded in obtaining the highest emission intensity of all the prepared samples in sample c, prepared under mild conditions, although these relative intensities should be compared carefully by taking into account the effect of the particle sizes on the apparent intensities. In our previous report,[40] the dispersion stability maintained by the treatment under mild conditions would allow the zeolite nanocrystallites to disperse homogeneously in organic solvent and to emit with the highest quantum efficiency.

As shown in Fig. 5(a), the bandwidth of the high-resolution emission spectrum of sample c was very sharp. The ratio of FWHM of the $^4F_{3/2}$–$^4I_{11/2}$ transition of the sample against the glass matrix, LHG-8, was 0.55. Therefore, the environment around Nd^{3+} within the zeolite should be more homogeneous than that in the glass matrix. This result reflects the high crystallinity of the zeolite. In the excitation spectrum of sample c shown in Fig. 5(b), the transition to the $^2P_{1/2}$ level split into the two bands. Since the $^2P_{1/2}$ level is not generally affected by the symmetry of the ligand field around the ion, at least two different chemical components of Nd^{3+} ions are considered to exist. Taking into consideration that the PMS/Nd^{3+} ratio was 1.5 (see Table 1), the two components should be $[Nd(PMS)]^{2+}$, and $[Nd(PMS)_2]^+$ with the excess positive charge balanced by the negative charge of the zeolite framework.

III. Diffuse reflectance spectra

A. Behavior of O–H vibration. The changes in the intensity of the O–H stretching vibration ($v = 2$) were traced with the DR spectra of Nd^{3+}-exchanged TMA–nano-FAU zeolites prepared under different conditions, as depicted in Fig. 6. In the DR spectra, a broad band with very high intensity was observed at 1400 nm (7100 cm^{-1}), assigned to the O–H stretching vibration ($v = 2$). The band intensity decreased upon heating at 423 K. For the samples treated by degassing and

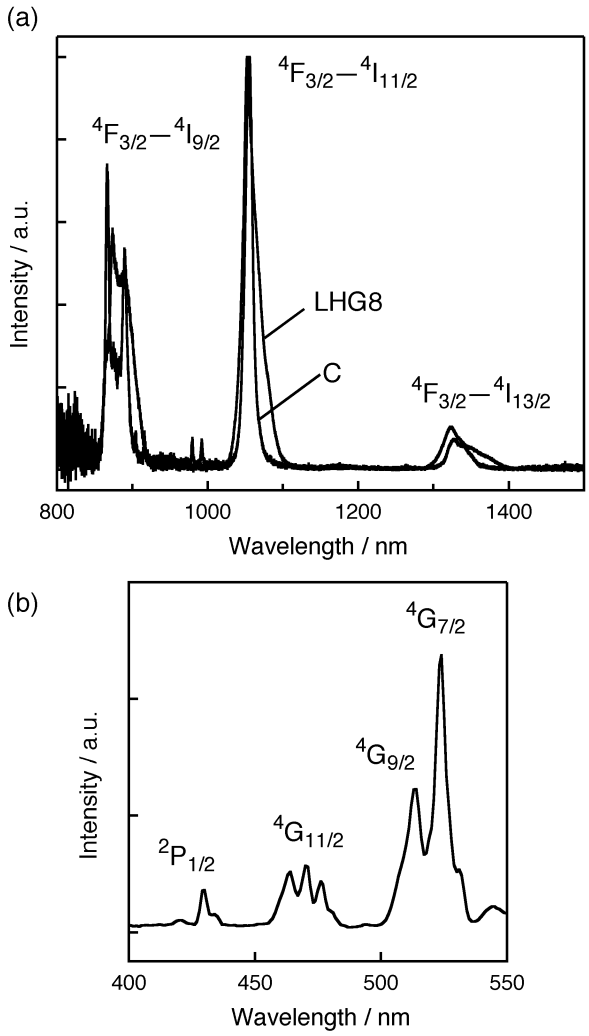

Fig. 5 The high resolution (a) emission and (b) excitation spectra of Nd^{3+}-exchanged TMA–nano-FAU degassed at 423 K, kept in contact with PMS vapor, and then degassed at 423 K (sample c).

deuteration (sample a and b), the intensity decreased markedly compared to the hydrated sample. However, these samples gave no emission as demonstrated in Table 1 and Fig. 3. The excited states of Nd^{3+} ions should be also quenched by the residual O–H groups. Also, it is likely that the excited states should be quenched by coordinating heavy water or O–D groups because there has been no successful example of observing emission of Nd^{3+} in heavy water, except under laser excitation.[11] Although the intensity of the O–H stretching vibration for TMA–nano-FAU treated with PMS and heated at 423 K (sample c) was larger than those of the heated and deuterated zeolites, this zeolite showed the strongest emission. Since the Nd^{3+} ion ligated by PMS emitted even if O–H groups remained in the zeolite lattice, we concluded that the ligands should eliminate O–H groups from the vicinity of Nd^{3+} ions.

B. Judd–Ofelt analysis. Judd–Ofelt analysis is difficult by using diffusion reflectance spectra because the optical pathlength of the sample is necessary, as described in the experimental section. We obtained Ω_t ($t = 2$, 4 and 6) parameters as relative values by calculation under the assumption that the optical pathlength was 0.01 cm. Changes in the Ω_t ($t = 2, 4$ and 6) parameters obtained in the Judd–Ofelt analysis arise from the ligand field and chemical bonding properties around the Nd^{3+} center. The Ω_2 parameter is particularly sensitive to changes in the ligand field, and a more asymmetric ligand field results in a greater increase in Ω_2.[41]

Fig. 7 shows plots of the Ω_2 value *versus* the treatment

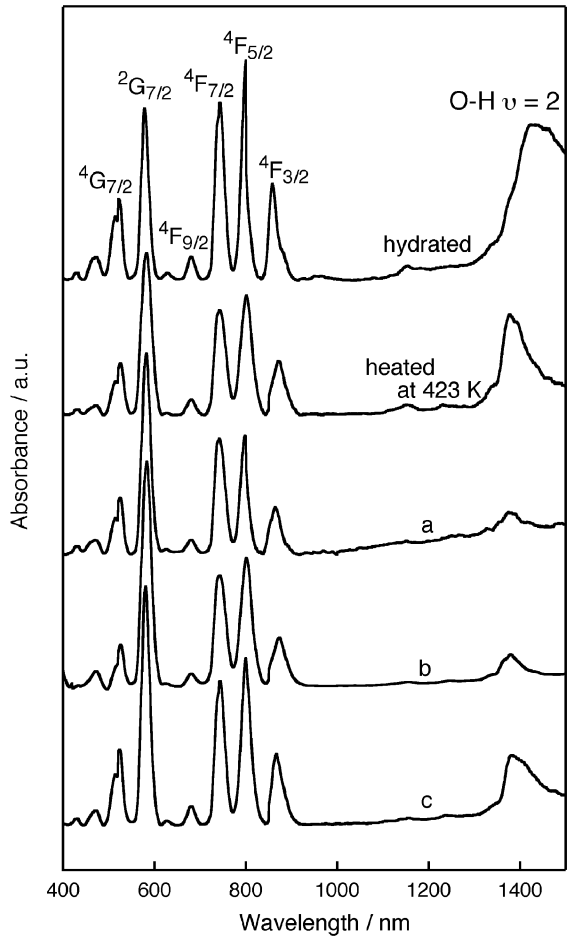

Fig. 6 Diffuse reflectance spectra of Nd^{3+}-exchanged TMA–nano-FAU zeolites prepared under different conditions. The sample names are listed in Table 1.

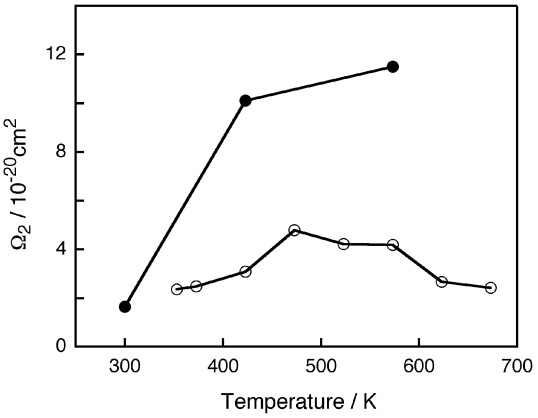

Fig. 7 Changes in the Ω_2 value of Nd^{3+}-exchanged zeolites heated at different temperatures: TMA–nano-FAU (closed circles), Na–micro-FAU (open circles).

temperature. Three different regions can be distinguished for Na–micro-FAU zeolite. The value first increased up to 473 K (region 1) and then a decrease was observed between 473 and 623 K (region 2). Finally, the value remained almost unchanged from 623 K to 673 K (region 3). Thus, it is most likely that the site symmetry of the cation was gradually lowered in region 1, but it became higher in region 2. In addition, the constant value in region 3 reveals that no further variation in the site symmetry was induced by the thermal treatment in this temperature region. Just after the ion exchange, rare-earth ions are speculated to occupy site V in the supercage (see Fig. 1(a)) with eight or nine coordinating waters, experiencing a high symmetric ligand field.[26,43] The ideal symmetries of site I′ in the sodalite cage and site I in the hexagonal prism are C_{3v} and O_h, respectively.[26] The symmetry of O_h is higher than that of C_{3v}. Thus, the changes in the Ω_2 value depending on the treatment temperatures for Na–micro-FAU zeolite show that Nd^{3+} ions migrate from the supercages to the sodalite cages in temperature region 1 and from the sodalite cages to the hexagonal prisms in region 2, and stay at site I in region 3. Hong *et al.* reported an analogous change of the symmetry around Tb^{3+} ions in Tb^{3+}-exchanged FAU zeolite depending on the thermal treatment.[26]

Emission was observed at first once the treatment temperature was raised to over 473 K, in which the Ω_2 value reached a maximum. This suggests that Nd^{3+} can emit when the ion occupies site I in the hexagonal prism. In the case of Tb^{3+} or Eu^{3+}-exchanged FAU zeolites, these ions emit effectively even at site I′ in the sodalite cages[26,33] because the numbers of coordinating waters decrease to one.[44] The excited state of Nd^{3+} in this site would be quenched by this residual coordinating water because the energy transfer through vibrational excitation to O–H groups is more effective for Nd^{3+} than for Tb^{3+} or Eu^{3+}.[11] Probably, the luminescence can be observed since Nd^{3+} ions located in site I have no coordinating water.

The change in the Ω_2 values of Nd^{3+}-exchanged TMA–nano-FAU zeolites induced by the thermal treatment was quite different from that of Na–micro-FAU zeolites. The Ω_2 values increased without a maximum, as the temperature of the thermal treatment became higher. The coordinating waters can be eliminated by the thermal treatment without migrating to the inner sites of the zeolite because of occupancy of TMA^+ in the sodalite cage. The removal of coordinating water would cause the low symmetry ligand field. If the Nd^{3+} ions are still placed in the supercages, the site symmetry of the ion distorted by water loss could be restored to the original state by subsequent rehydration. We confirmed the recovery of the Ω_2 values of the samples treated at 423 and 573 K by rehydration.

The strongest luminescence was not obtained by thermal treatment at high temperatures but obtained by the treatment with PMS in TMA–nano-FAU zeolite, in contrast to the case of Na–micro-FAU zeolite. This is explained as due to whether Nd^{3+} ion migration into the inner cages occurs or not. Since the ligand, PMS, cannot penetrate into the sodalite cages but can into the supercages, the ligation of PMS to Nd^{3+} would be achieved more easily in TMA–nano-FAU than in Na–micro-FAU zeolite. This is confirmed by the large change in the Ω_2 value of TMA–nano-FAU before and after the treatment with PMS, in contrast to the small change in the value of Na–micro-FAU (see Table 3). TMA^+-containing FAU zeolite could be a suitable host for ship-in-bottle synthesis of metal complexes.

The Ω_2 value of TMA–nano-FAU heated at 573 K after the treatment with PMS (sample d) is intermediate between those of the zeolites heated at 573 K (sample b) and sample c (see Table 3). The content of the adsorbed ligand in sample d was lower than that in sample c. So, it is suggested that the low emission intensity of this sample should be caused by bare

Table 3 Judd–Ofelt parameters of Nd^{3+}-exchanged zeolites prepared under different conditions

		J–O parameter/10^{-20} cm^2		
Sample	Type of zeolite	Ω_2	Ω_4	Ω_6
a	TMA–nano	10.1	6.48	9.79
b	TMA–nano	11.5	8.68	12.3
c	TMA–nano	6.20	15.7	12.3
d	TMA–nano	9.81	8.33	10.8
e	TMA–nano	2.10	11.3	9.33
f	Na–micro	3.08	9.54	7.56
l	Na–micro	2.10	6.21	5.19

Nd^{3+} ions similar to the ones in sample b, which are generated by thermal removal of the ligands.

Conclusions

We have succeeded in producing a strong luminescent Nd^{3+}-exchanged zeolite by using TMA^{+}-containing FAU zeolite nanocrystallites as a host matrix and bis(perfluoromethanesulfonyl)aminate (PMS) as a low vibrational ligand of the ion under mild conditions. The facility of the ligation of PMS with the ions in the cage of the zeolite and the protection effect of the ligand against OH groups present in the pores of the zeolite brought about the strong emission intensity. The ease of the ligation was caused by the Nd^{3+} ions residing in the supercages without cation migration into the inner cages. On the other hand, in Nd^{3+}-exchanged Na–micro-FAU zeolite, the higher thermal treatment resulted in the more effective emission because of the occurrence of cation migration to the inner cages, while the treatment with PMS induced only weak luminescence.

Acknowledgement

The authors are grateful to Mr. S. Shirato and Dr. J. Prevelt for their discussions. We would also like to thank the members of the Institute of Laser Engineering, Osaka University for help with the spectral measurements in the near IR-region. This work was, in part, supported by the "Research for the Future" Program, JSPS No. 96P00305, and a Grant-in-Aid for Scientific Research from the Ministry of Education, Science, Sports, and Culture of Japan. We also thank the Asahi Glass Foundation for their financial support.

References

1 B. Whittaker, *Nature*, 1970, **288**, 157.
2 K. Kuriki, S. Nishihara, Y. Nishizawa, A. Tagaya, Y. Koike and Y. Okamoto, *Electron. Lett.*, 2001, **37**, 415.
3 Y. Kawamura, Y. Wada, Y. Hasegawa, M. Iwamuro, T. Kitamura and S. Yanagida, *Appl. Phys. Lett.*, 1999, **74**, 3245.
4 A. Heller, *J. Am. Chem. Soc.*, 1966, **88**, 2058.
5 Y. Haas and G. Stein, *J. Phys. Chem.*, 1971, **75**, 3677.
6 Y. Haas, G. Stein and E. Würzberg, *J. Chem. Phys.*, 1974, **60**, 258.
7 U. Gösele, M. Hauser, U. K. A. Klein and R. Frey, *Chem. Phys. Lett.*, 1975, **34**, 519.
8 U. Gösele, *Chem. Phys. Lett.*, 1976, **43**, 61.
9 J. A. Caird, A. J. Ramponi and P. R. Staver, *J. Opt. Soc. Am. B*, 1991, **8**, 1391.
10 A. Heller, *J. Am. Chem. Soc.*, 1967, **89**, 167.
11 A. Beeby and S. Faulkner, *Chem. Phys. Lett.*, 1997, **266**, 116.
12 Y. Hasegawa, K. Murakoshi, Y. Wada, S. Yanagida, J.-H. Kim, N. Nakashima and T. Yamanaka, *Chem. Phys. Lett.*, 1996, **248**, 8.
13 Y. Hasegawa, Y. Kimura, K. Murakoshi, Y. Wada, T. Yamanaka, J.-H. Kim, N. Nakashima, T. Yamanaka and S. Yanagida, *J. Phys. Chem.*, 1996, **100**, 10201.
14 Y. Hasegawa, K. Murakoshi, Y. Wada, T. Yamanaka, J.-H. Kim, N. Nakashima, T. Yamanaka and S. Yanagida, *Chem. Phys. Lett.*, 1996, **260**, 173.
15 Y. Hasegawa, T. Ohkubo, K. Sogabe, Y. Kawamura, Y. Wada, N. Nakashima and S. Yanagida, *Angew. Chem., Int. Ed.*, 2000, **39**, 357.
16 M. Borja and P. K. Dütta, *Nature*, 1993, **362**, 43.
17 M. Sykora and J. R. Kincaid, *Nature*, 1997, **387**, 162.
18 J. C. Scaiano and H. Garcia, *Acc. Chem. Res.*, 1999, **32**, 783.
19 V. Ramamuthy, D. F. Eaton and J. V. Caspar, *Acc. Chem. Res.*, 1992, **25**, 299.
20 S. D. Cox, T. E. Gier, G. D. Stucky and J. Bierlein, *J. Am. Chem. Soc.*, 1988, **110**, 2986.
21 G. Ihlein, F. Schüth, O. Krauβ, U. Vietze and F. Laeri, *Adv. Mater.*, 1998, **10**, 1117.
22 T. Arakawa, M. Takakuwa, G.-y. Adachi and J. Shiokawa, *Bull. Chem. Soc. Jpn.*, 1984, **57**, 1290.
23 B. L. Benedict and A. B. Ellis, *Tetrahedron*, 1987, **43**, 1625.
24 J. R. Bartlett, R. P. cooney and R. A. Kydd, *J. Catal.*, 1988, **114**, 58.
25 M. F. Hazenkamp, A. M. H. v. d. Veen, N. Feiken and G. Blasse, *J. Chem. Soc., Faraday. Trans.*, 1992, **88**, 141.
26 S. B. Hong, J. S. Seo, C.-H. Pyun, C.-H. Kim and Y. S. Uh, *Catal. Lett.*, 1995, **30**, 87–97.
27 S. Lee, H. Hwang, P. Kim and D. Jang, *Catal. Lett.*, 1999, **57**, 221.
28 M. D. Baker, M. M. Olken and G. A. Ozin, *J. Am. Chem. Soc.*, 1988, **110**, 5709.
29 U. Kynast and V. Weiler, *Adv. Mater.*, 1994, **6**, 937.
30 I. L. V. Rosa, O. A. Serra and E. J. Nassar, *J. Lumin.*, 1997, **72**, 532.
31 M. Alvaro, V. Fornes, S. Garcia and H. G. J. C. Scaiano, *J. Phys. Chem. B*, 1998, **102**, 8744.
32 C. Borgmann, J. Sauer, T. Jüstel, U. Kynast and F. Schüth, *Adv. Mater.*, 1999, **11**, 45.
33 W. Chen, R. Samynaiken and Y. Huang, *J. Appl. Phys.*, 2000, **88**, 1424.
34 J. Rocha, L. D. Carlos, J. P. Rainho, Z. Lin, P. Ferreira and R. M. Almedia, *J. Mater. Chem.*, 2000, **10**, 1371.
35 T. Jüstel, D. U. Wiechert, C. Lau, D. Sendor and U. Kynast, *Adv. Funct. Mater.*, 2001, **11**, 105.
36 B. J. Schoeman, J. Sterte and J.-E. Otterstedt, *Zeolites*, 1994, **14**, 110.
37 N. B. Castagnola and P. Dutta, *J. Phys. Chem. B*, 1998, **102**, 1696.
38 M. Tsapatsis, M. Lovallo, T. Okubo, M. E. Davis and M. Sadakata, *Chem. Mater.*, 1995, **7**, 1734.
39 G. Zhu, S. Qui, J. Yu, Y. Sakamoto, F. Xiao, R. Xu and O. Terasaki, *Chem. Mater.*, 1998, **10**, 1483.
40 Y. Wada, T. Okubo, M. Ryo, T. Nakazawa, Y. Hasegawa and S. Yanagida, *J. Am. Chem. Soc.*, 2000, **122**, 8583.
41 M. Iwamuro, Y. Hasegawa, Y. Wada, K. Murakoshi, N. Nakashima, T. Yamanaka and S. Yanagida, *J. Lumin.*, 1998, **79**, 29 and references therein.
42 L. S. d. Saldarriaga, C. Saldarriaga and M. E. Davis, *J. Am. Chem. Soc.*, 1987, **109**, 2686.
43 J. F. Taguay and S. L. Suib, *Catal. Rev. Sci. Eng.*, 1987, **29**, 1.
44 M. L. Costenoble, W. J. Mortier and J. B. Uytterhoeven, *J. Chem. Soc., Faraday. Trans.*, 1978, **74**, 466.